Modelling of high-numerical-aperture imaging of complex scatterers using T-matrix method

V. L. Y. Loke[1,2], T. A. Nieminen[1,*], N. R. Heckenberg[1], and H. Rubinsztein-Dunlop[1]

[1]*The Univ. of Queensland, Quantum Science Lab., Sch. of Math. and Phys., QLD 4072, Australia.*
[2]*Özyeğin University, School of Engineering, Altunizade, Istanbul, Turkey.*

A high-numerical-aperture objective used for imaging can be represented by a T-matrix. Thus, it is possible to model the imaging of complex objects that can be themselves modelling using the T-matrix method. Polarization filtering can be included.

INTRODUCTION

The imaging of microscopic objects is a commonly performed optical task using a standard optical instrument, the optical microscope. An elementary treatment of microscopy is included in the typical optics course or textbook, so it would be reasonable to assume that the calculation or modelling of image formation is straightforward. However, the usual treatment of the problem is based on a number of simplifying assumptions, such as the paraxial and scalar approximations [1]. While it is possible to reduce the number of approximations, for example by using nonparaxial 3D vectorial transfer functions [2], the treatment of complex objects, where multiple scattering within the object being imaged is important, such as will be the case for thick objects, or polarization effects are important, remains an outstanding problem, especially for high-numerical-aperture imaging (e.g., beyond NA ≈ 1 for water- or oil-immersion objectives, or NA ≈ 0.75 in air).

We will consider a simple treatment of high-numerical-aperture vectorial imaging, with full polarization effects, of an arbitrary complex object. We will assume that an existing method can be used for calculating the field scattered from the object of interest, at an arbitrary point in space. We will assume that this information is available in the form of a T-matrix of the object; in principle, this can be obtained using whatever method of choice is used for the actual scattering calculation [3, 4].

Note that knowledge of the scattered field does not immediately allow us to determine the image captured by the objective lens of a microscope, which has a limited field of view and is focused on a given horizontal plane that intersects the particle. It is necessary to first determine what part of the scattered field of the object being imaged is collected and focussed. Here, we present a method, using the T-matrix formulation, for reproducing the image seen through a high numerical aperture microscope imaging system, motivated by our recent experimental work on polarization imaging of microscopic vaterite spherulites [5].

METHOD

The fields of the incident ($\mathbf{E}_{inc}$) and scattered ($\mathbf{E}_{sca}$) light for an illuminated particle can be represented in terms of vector spherical wave functions (VSWFs) [6, 3, 4, 7]:

*Corresponding author: Timo Nieminen (timo@physics.uq.edu.au)

$$\mathbf{E}_{\text{inc}} = \sum_{n=1}^{\infty} \sum_{m=-n}^{n} a_{nm}\mathbf{M}_{nm}^{(3)}(kr) + b_{nm}\mathbf{N}_{nm}^{(3)}(kr), \tag{1}$$

$$\mathbf{E}_{\text{sca}} = \sum_{n=1}^{\infty} \sum_{m=-n}^{n} p_{nm}\mathbf{M}_{nm}^{(1)}(kr) + q_{nm}\mathbf{N}_{nm}^{(1)}(kr). \tag{2}$$

where $\mathbf{M}_{nm}^{(3)}$ and $\mathbf{N}_{nm}^{(3)}$ are regular VSWFs, $\mathbf{M}_{nm}^{(1)}$ and $\mathbf{N}_{nm}^{(1)}$ are the outward-propagating VSWFs, n and m are radial and azimuthal mode indices respectively and the coefficients of the incident and scattered fields are related by the T-matrix [6, 3, 4]:

$$\begin{bmatrix} p_{nm} \\ q_{nm} \end{bmatrix} = \mathbf{T} \begin{bmatrix} a_{nm} \\ b_{nm} \end{bmatrix}. \tag{3}$$

The light scattering properties of the particle, for a given wavelength, are expressed in the T-matrix.

The same formalism can be used to represent the effect of the imaging objective. In this case, our coefficients a_{nm} and b_{nm} are the coefficients of the total outgoing field from the object (that is, the sum of the outgoing portion of the incident field, which could, for example, be a plane wave or a focussed beam, and the scattered field), and p_{nm} and q_{nm} are the part of this outgoing field collected by the objective.

Firstly, we calculate the scattering coefficient as per the canonical T-matrix method using (3). We used the T-matrix for the object (here, this is a vaterite sphere, and we calculate the T-matrix using a hybrid FDTD/T-matrix method [8]).

We then cycle through all the azimuthal and radial modes (m and n) incident on the objective, one at a time, finding the spherical wave spectrum of the collected field using over-determined least-squares point-matching [3]. The objective is in the far-field of the light from the object, and the only parameter needed to represent the objective is the angles over which light enters (determined from the numerical aperture). The size of the region being viewed determines the series truncation: $n = N_{max} \approx x$, where x is the "size parameter" or the viewed area. The effective radius of this area is that, measured from the focal point of the objective, required to enclose the object. For a sub-resolution object, the resolution limit should be used as the effective size. Each iteration yields a column of the T-matrix describing the objective. For a simple rotationally symmetric objective, there will be no coupling to different values of m, as usual for the T-matrix for axisymmetric objects [6, 3, 9].

If a polarizer is included in the objective system, e.g., for viewing a sample through crossed polarizers, there will be coupling between different angular momenta, and the usual optimisation for axisymmetric particles can no longer be used. However, this coupling is highly restricted, and only a limited subset of angular momenta are available, so it is still possible to optimise this calculation, as described in the following section.

In effect, we use a double T-matrix method, involving using the pre-calculated T-matrix of the scatterer in free space, and a T-matrix representing the effect of the objective (and polarizer, if included). The T-matrix for the objective does not depend on the object being imaged, and can be calculated independently, and the same T-matrix used for the imaging of a variety of objects.

Effect of polarizer

The VSWFs expansions used in (1) and (2) to represent the electromagnetic fields are in spherical polar coordinates. The filter can be represented as a matrix applied to the outgoing field, in spherical coordinates. The radial component ($\mathbf{E}_r$) can be ignored as it approaches zero in far-field; thus, the filter matrix dimensions will be 2×2. For our derivation of the filter matrix, the beam is linearly polarized in the x-direction and propagates in the $+z$-direction. The cross-polarization filter sits flat on the horizontal plane and it filters out the y-component of the $\mathbf{E}$-field.

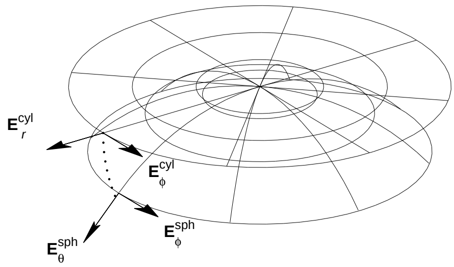

Figure 1. Projecting the E-field vectors from the spherical to the cylindrical coordinate system.

Consider the x-component of the filtered $\mathbf{E}$-field expressed in cylindrical coordinates,

$$\mathbf{E}_x = \mathbf{E}_r^{(cyl)} \cos \phi_{cyl} - \mathbf{E}_\phi^{(cyl)} \sin \phi_{cyl}, \tag{4}$$

and $\mathbf{E}_y = 0$. Since the fields are calculated in spherical coordinates, we project the spherical components onto the cylindrical plane (figure 1) such that $\mathbf{E}_\phi^{(sph)} \to \mathbf{E}_\theta^{(cyl)}$ and $\mathbf{E}_\theta^{(sph)} \to \mathbf{E}_r^{(cyl)}$, when substituted in (4), the field components expressed in spherical coordinates and in matrix form is

$$\begin{bmatrix} \mathbf{E}_x \\ 0 \end{bmatrix} = \begin{bmatrix} \cos\phi & -\sin\phi \\ 0 & 0 \end{bmatrix} \begin{bmatrix} \mathbf{E}_\theta \\ \mathbf{E}_\phi \end{bmatrix}, \tag{5}$$

bearing in mind that $\phi_{sph} = \phi_{cyl}$. Now, converting back to spherical coordinates,

$$\begin{bmatrix} \mathbf{E}'_\theta \\ \mathbf{E}'_\phi \end{bmatrix} = \begin{bmatrix} \cos\phi & \sin\phi \\ -\sin\phi & \cos\phi \end{bmatrix} \begin{bmatrix} \cos\phi & -\sin\phi \\ 0 & 0 \end{bmatrix} \begin{bmatrix} \mathbf{E}_\theta \\ \mathbf{E}_\phi \end{bmatrix}, \tag{6}$$

we obtain the filter matrix in the spherical coordinate system,

$$\begin{bmatrix} \mathbf{E}'_\theta \\ \mathbf{E}'_\phi \end{bmatrix} = \begin{bmatrix} \cos^2\phi & -\cos\phi\sin\phi \\ -\cos\phi\sin\phi & \sin^2\phi \end{bmatrix} \begin{bmatrix} \mathbf{E}_\theta \\ \mathbf{E}_\phi \end{bmatrix}. \tag{7}$$

RESULTS AND DISCUSSION

The method was tested using an object composed of four square slabs, shown on the left in figure 2, with resolution consistent with the Rayleigh criterion and polarization effects. On the right, figure 2 shows calculated images of a vaterite microsphere compared with experimental results [5].

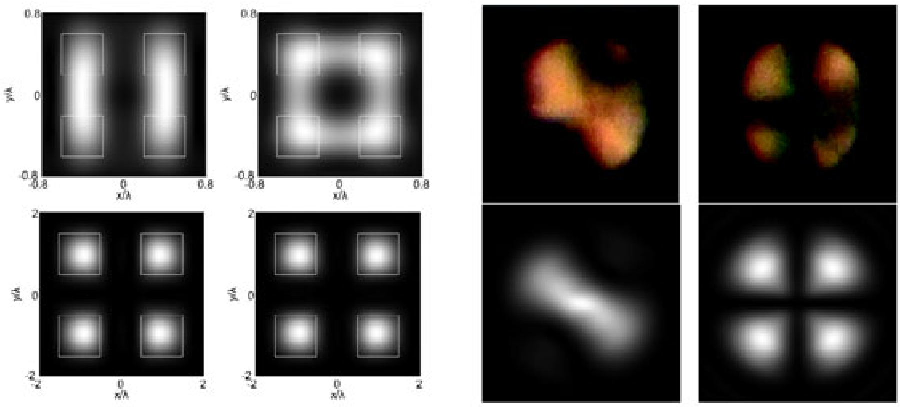

Figure 2. **Left:** Imaging of four square objects. Squares in the top row are 0.4λ across, and in the bottom row, 1λ. The illumination plane-polarized in the up--down direction in the left column, and circularly polarized on the right. **Right:** Experimental (top) and calculated (bottom) images of vaterite microspheres as seen through crossed polarizers.

Overall, it can be seen that the method works, even for complex objects that strongly affect the polarization of the light. By exploiting the mirror symmetry of the polarizer when solving the linear system resulting from the point-matching, the calculation of the T-matrix of the imaging system took a matter of minutes on a high-end desktop PC.

Although it is possible to include interaction (i.e., multiple scattering) between the objective and the object, e.g., iteratively, we have not done so here since the large distance between them, and the design of the objective to limit reflection (or back-scattering) makes this unnecessary for imaging applications.

REFERENCES

[1] C. J. R. Sheppard. The optics of microscopy. J. Opt. A **9** (2007).

[2] M. R. Arnison and C. J. R. Sheppard. A 3D vectorial optical transfer function suitable for arbitrary pupil functions. Opt. Commun. bf 211 (2002).

[3] T. A. Nieminen, H. Rubinsztein-Dunlop, and N. R. Heckenberg. Calculation of the *T*-matrix: general considerations and application of the point-matching method. J. Quant. Spectrosc. Radiat. Transfer **79--80** (2003).

[4] F. M. Kahnert. Numerical methods in electromagnetic scattering theory. J. Quant. Spectrosc. Radiat. Transfer **79--80** (2003).

[5] S. J. Parkin et al. Highly birefringent vaterite microspheres: production, characterization and applications for optical micromanipulation. Opt. Express **17** (2009).

[6] P. C. Waterman. Symmetry, unitarity, and geometry in electromagnetic scattering. Phys. Rev. D **3** (1971).

[7] T. A. Nieminen, H. Rubinsztein-Dunlop, and N. R. Heckenberg. Multipole expansion of strongly focussed laser beams. J. Quant. Spectrosc. Radiat. Transfer **79--80** (2003).

[8] V. L. Y. Loke et al. FDFD/T-matrix hybrid method. J. Quant. Spectrosc. Radiat. Transfer **106** (2007).

[9] M. I. Mishchenko. Light scattering by randomly oriented axially symmetric particles. J. Opt. Soc. Am. A **8** (1991).